A&A 510, A14 (2010)
DOI: 10.1051/0004-6361/200913278

Astronomy & Astrophysics

Circumstellar H I and CO around the carbon stars V1942 Sagittarii and V Coronae Borealis

Y. Libert[1], E. Gérard[2], C. Thum[3], J. M. Winters[3], L. D. Matthews[4], and T. Le Bertre[1]

[1] LERMA, UMR 8112, Observatoire de Paris, 61 Av. de l'Observatoire, 75014 Paris, France
e-mail: Thibaut.LeBertre@obspm.fr
[2] GEPI, UMR 8111, Observatoire de Paris, 5 place J. Janssen, 92195 Meudon Cedex, France
[3] IRAM, 300 rue de la Piscine, 38406 St. Martin d'Hères, France
[4] MIT Haystack Observatory, Off Route 40, Westford, MA 01886, USA

Received 11 September 2009 / Accepted 20 October 2009

ABSTRACT

Context. The majority of stars that leave the main sequence are undergoing extensive mass loss, in particular during the asymptotic giant branch (AGB) phase of evolution. Observations show that the rate at which this phenomenon develops differs widely from source to source, so that the time-integrated mass loss as a function of the initial conditions (mass, metallicity, etc.) and of the stage of evolution is presently not well understood.
Aims. We investigate the mass loss history of AGB stars by observing the molecular and atomic emission of their circumstellar envelopes.
Methods. We selected two stars that are on the thermally pulsing phase of the AGB (TP-AGB) for which high quality data in both the CO rotation lines and the atomic hydrogen line at 21 cm could be obtained.
Results. A carbon star of the irregular variability type, V1942 Sgr, has a complex CO line profile that may originate in a long-lived wind of rate $\sim 10^{-7}$ $M_\odot\,\mathrm{yr}^{-1}$, and from a young ($\lesssim 10^4$ years) fast outflow of rate $\sim 5 \times 10^{-7}$ $M_\odot\,\mathrm{yr}^{-1}$. The intense H I emission is indicative of a detached shell with 0.044 $M_\odot$ of hydrogen. This shell probably results from the slowing-down, by surrounding matter, of the same long-lived wind observed in CO that has been active for $\sim 6 \times 10^5$ years. On the other hand, the carbon Mira V CrB is presently undergoing mass loss at a rate of 2×10^{-7} $M_\odot\,\mathrm{yr}^{-1}$, but was not detected in the H I data. The wind is mostly molecular and has been active for at most 3×10^4 years, with an integrated mass loss of at most 6.5×10^{-3} $M_\odot$.
Conclusions. Although both sources are carbon stars on the TP-AGB, they appear to develop mass loss in very different conditions, and a high rate of mass loss may not imply a high integrated mass loss.

Key words. stars: AGB and post-AGB – stars: carbon – circumstellar matter – stars: individual: V1942 Sagittarii – stars: individual: V Coronae Borealis

1. Introduction

Low- to intermediate-mass stars, at the end of their main-sequence evolution, become first hydrogen shell-burning red giants (RGB − red giant branch − stars), then hydrogen and helium shell-burning red giants (AGB − asymptotic giant branch − stars). In this second phase, they may undergo mass loss at a very high rate ($>10^{-8}$ $M_\odot\,\mathrm{yr}^{-1}$), sufficiently high to have a decisive effect upon their late evolution (Olofsson 1999). They are surrounded by expanding envelopes of gas and dust, which have been extensively observed with radio molecular lines and infrared continuum emission. These tracers are used to estimate mass-loss rates. However, the estimates are somewhat ambiguous because the mass-loss rate of a given source may vary on many different timescales. The change in mass as a function of time due to mass loss is thus difficult to evaluate, and to relate to stellar evolution models. Furthermore, molecular lines probe an extent of the circumstellar shell (CS) that is limited by photodissociation, and therefore provide information mainly about the inner parts of CSs, and on the recent mass loss.

To try to circumvent these difficulties, we have started a systematic program of observations of red giants in the line of atomic hydrogen at 21 cm. We have published some of our results in several recent papers, and the first reports for sizeable samples were presented by Gérard & Le Bertre (2006, hereafter GL2006) and Matthews & Reid (2007, hereafter MR2007). A major difficulty of this program is the confusion caused by the 21 cm emission from the interstellar medium (ISM) located along the same line-of-sight as the source of interest. This has a strong impact on the observations, which must be conducted using a specific approach, and on the data processing that aims to provide spectra corrected for ISM emission. Furthermore, since circumstellar matter is expected to be at some stage injected into the ISM, the confusion by the local ISM might actually be partly of stellar origin, i.e., caused by material ejected at an earlier stage of evolution.

In addition to observing the H I line at 21 cm systematically in a large number of sources with different properties, it is also important to choose objects for which the Galactic confusion is low and/or can be tracked easily, and therefore corrected accurately. The detailed study of these spectra should serve as a guide to exploit the data that are obtained in more difficult situations.

Here we present our results for two carbon stars, V1942 Sgr and V CrB, for which the confusion is not a serious problem, and which have H I properties that differ radically. Both are N-type carbon stars (CGCS 4229 and CGCS 3652, respectively) that have already been detected in CO rotational lines (Olofsson et al. 1993a). However, the only previously available CO spectrum of

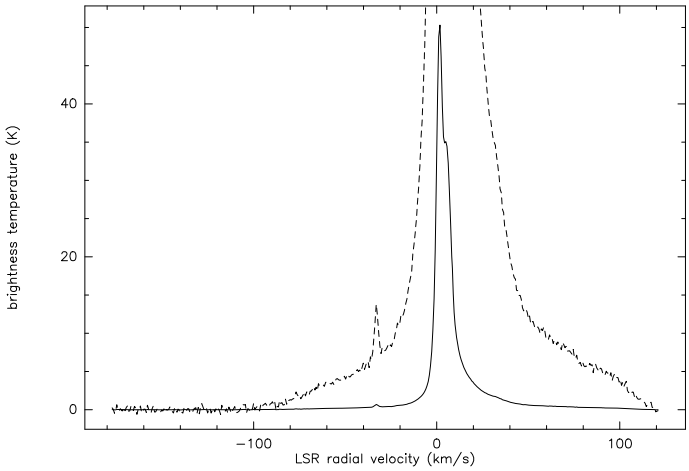

Fig. 1. Frequency-switched H I 21 cm spectrum obtained with the NRT on the position of V1942 Sgr. The spectrum enlarged by a factor 20 is also shown as a dashed line. The emission from V1942 Sgr is clearly detected at −33 km s^{-1}.

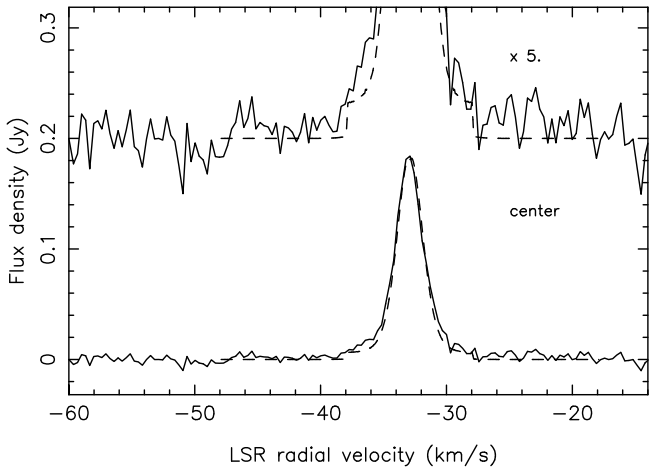

Fig. 2. H I line profile of V1942 Sgr. The spectrum has been smoothed to a resolution of 0.32 km s^{-1}. The dashed line is a fit obtained with the model described in Sect. 4.1.

V1942 Sgr had been of low signal-to-noise ratio, and for our study it appeared essential to also obtain new CO data of high quality.

2. V1942 Sgr

V1942 Sgr is classified as a long-period irregular variable (type Lb). Lebzelter & Obbrugger (2009) compared the light-curve properties of semi-regular (SR) and Lb variables, and concluded that Lb stars can be seen as an extension of the SRs that have shorter periods and smaller amplitudes. V1942 Sgr is a carbon star on the TP-AGB with a C/O ratio of around 1.12 (Olofsson et al. 1993b). Bergeat et al. (2001) estimate that its effective temperature, $T_{\rm eff}$, is 2960 K. The parallax measured by Hipparcos (1.87 ± 0.51 mas, van Leeuwen 2007) places it at 535 pc, implying a luminosity of 5200 $L_{\odot}$. From the data obtained by IRAS in the mid-infrared, there is no direct evidence that the star is undergoing mass loss (the low resolution 8–22 μm spectrum is featureless). However, Olofsson et al. (1993a) discovered emission in the CO(1–0) rotational line centered on $V_{\rm lsr}$ = −31.5 km s^{-1}, close to the expected radial velocity of V1942 Sgr ($V_{\rm lsr}$ = −32.0 km s^{-1} from the General Catalogue of Stellar Radial Velocities). The expansion velocity, $V_{\rm exp}$ = 12.4 km s^{-1}, is surprisingly high for an Lb variable. From this spectrum, Schöier & Olofsson (2001) derive a mass-loss rate of ∼2.5 × 10^{-7} $M_{\odot}$ yr^{-1} (at 535 pc). Extended emission associated with V1942 Sgr was discovered by IRAS (Young et al. 1993a). The 60 μm data show a resolved shell of external radius 3.2′, i.e., 0.50 pc.

2.1. H I observations

The H I emission was observed with the Nançay Radio Telescope (NRT), between March 2007 and July 2009, for a total of 85 h. The NRT beamwidth (*FWHM*) at 21 cm is 4′ in right ascension (RA) and 22′ in declination (Dec). An on-source frequency-switched spectrum is presented in Fig. 1. The main emission peaks at 50 K around $V_{\rm lsr}$ = 0 km s^{-1}. A narrow emission feature with a peak of ∼0.3 K, centered on −33 km s^{-1}, is visible on top of the 0.4 K blue wing of the main peak near 0 km s^{-1}.

Position-switched spectra were also obtained with an on-position taken at the position of V1942 Sgr and off-positions, at ±2′, ±4′, ±6′, ±8′, ±10′, ±12′, ±16′, ±24′, and ±32′. The comparison between the spectra obtained for different values of the throw shows that the interstellar emission varies linearly with offset in the velocity range from −100 to −20 km s^{-1}. It means that the H I background emission around V1942 Sgr shows a gradient in RA that is constant for each velocity. This situation is similar to that encountered for EP Aqr and Y CVn (Le Bertre & Gérard 2004, Figs. 3 and 7). In such a case, the source emission can be extracted from the position-switched spectra by subtracting the contribution of the interstellar emission, which is estimated by interpolation between the two extreme off-positions.

The intensity of the emission detected from the source in the position-switched spectra is constant with throw from ±4′ to ±32′. Therefore, the source is confined mostly to the central beam (i.e., ±2′ in RA; see GL2006, Sect. 2.1). The spectrum obtained at the star's position is shown in Fig. 2. It has a shape similar to that obtained for Y CVn (Libert et al. 2007) with a narrow emission line superimposed on a pedestal extending from −39 to −27 km s^{-1}. The narrow emission is centered on $V_{\rm lsr}$ = −32.9 km s^{-1} and has a quasi-Gaussian profile of width 2.95 km s^{-1} (*FWHM*) and peak intensity 168 mJy. The pedestal is also centered on ∼−33 km s^{-1} and has an intensity of ∼6 ± 2 mJy. The peak intensity at the central position (178 mJy) agrees with that measured in the frequency-switched spectrum (cf. Fig. 1, with a conversion factor of 2.15 K/Jy for the NRT at 21 cm). We also searched for H I emission at blueshifted velocities as low as −48 km s^{-1}, and redshifted velocities as high as −18 km s^{-1} (see the CO spectra in Sect. 2.2). We set an upper limit of 2 mJy on emission over this range. Nevertheless, we suspect that there are residual features at −46, −26, and −24 km s^{-1}, possibly peaking at ∼3 mJy.

The spectra of the source in the off-positions are then determined by subtracting the individual position-switched spectra (on-off) and the contribution of the interstellar emission (assuming that it varies linearly with RA) from the central spectrum. Furthermore, we obtained data for on-positions at 11′ north and 11′ south, and off-positions at ±2′, ±4′, and ±12′, and then on-positions at 22′ north and 22′ south, and off-positions at ±8′. All of these data were used to construct the flux density map of the source presented in Fig. 3.

In this map, we see that the intensity at −2′ west is almost the same as on the star, and therefore conclude that the source is slightly offset west from the stellar position. Assuming

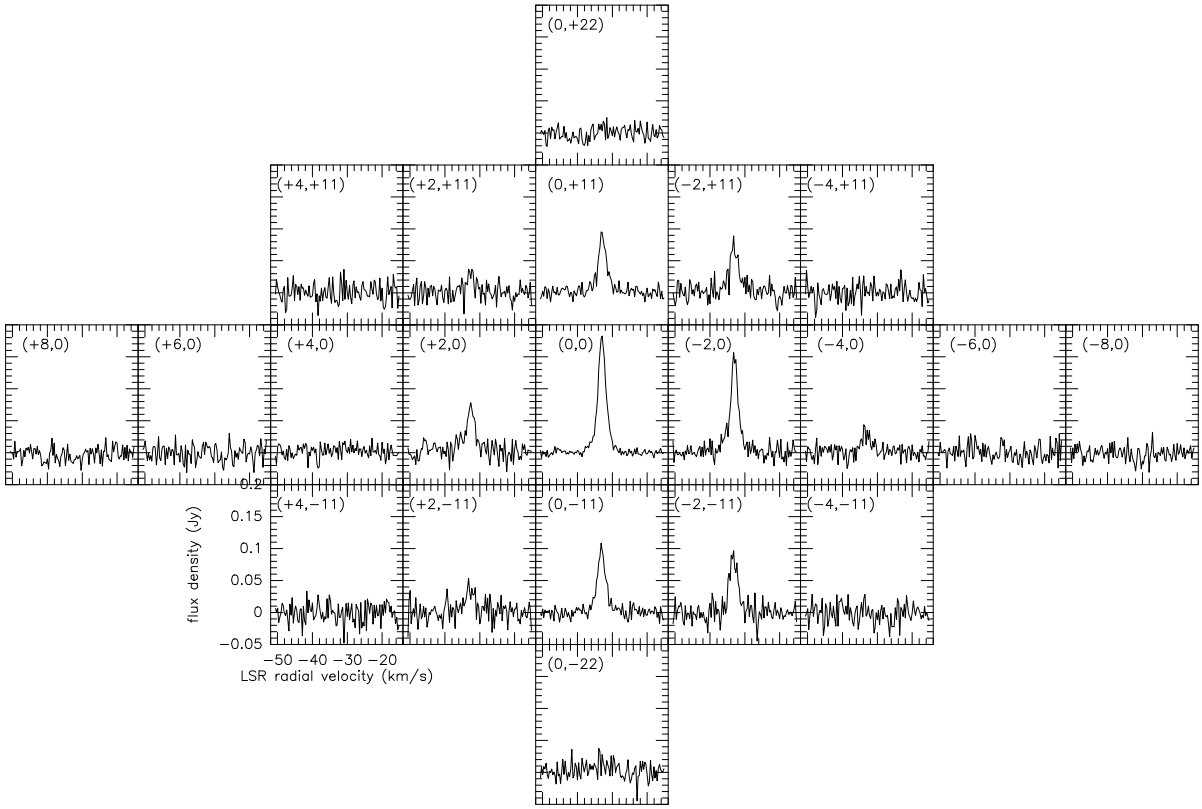

Fig. 3. Map of the 21 cm H I emission of V1942 Sgr. In each box, the label at upper left indicates the position (RA, Dec) with respect to the central star in arcminutes.

a Gaussian distribution of the intensity, we estimate that the H I source is centered on 0.6′ (±0.1′) west in RA and on 0′ (±1′) in Dec. The size (*FWHM*) would then be ∼1.3′ in RA and <5′ in Dec. The integrated flux in the map is 0.71 Jy × km s^{-1}. Assuming that the emission is optically thin and atomic hydrogen is at a temperature well above the background (≲0.4 K + 4.2 K, Reich & Reich 1986), and using the standard relation, $M_{\rm HI} = 2.36 \times 10^{-7} d^2 \int S_{\rm V} {\rm d}V$, with $M_{\rm HI}$ in $M_\odot$, d in pc, and $\int S_{\rm V} {\rm d}V$ in Jy × km s^{-1}, this flux translates to 0.048 $M_\odot$ of atomic hydrogen at 535 pc.

2.2. CO observations

CO observations of V1942 Sgr were obtained at the IRAM 30-m telescope equipped with the EMIR (Eight MIxer Receiver) on June 23, 2009 in average weather conditions (precipitable water vapor, pwv ∼10 mm). The two rotational lines, 1–0 and 2–1, were observed in parallel. The four EMIR bands were selected to detect the two orthogonal polarizations at 115.2712 and 230.5380 GHz ($T_{\rm sys}$ ∼ 400 K, ∼800 K, respectively). High spectral resolutions of 20 kHz and 40 kHz, respectively, (hence 0.05 km s^{-1}) were obtained with the VESPA (Versatile SPectrometer Array) backends. The telescope beamwidths are 21″ (at 115 GHz) and 11″ (at 230 GHz), and the observations were made in the wobbler-switching mode using a throw of 60″ in azimuth.

The spectra are shown in Fig. 4. These new spectra indicate that the line profiles are composite with two components centered on the same central velocity, but with different widths, similar to those observed by Knapp et al. (1998) and Winters et al. (2003) in several late-type giants, mostly oxygen-rich stars of the SR variability type. The emission extends from −48 to −18 km s^{-1}, and therefore we confirm the large expansion velocity (≳12 km s^{-1}) estimated by Olofsson et al. (1993a).

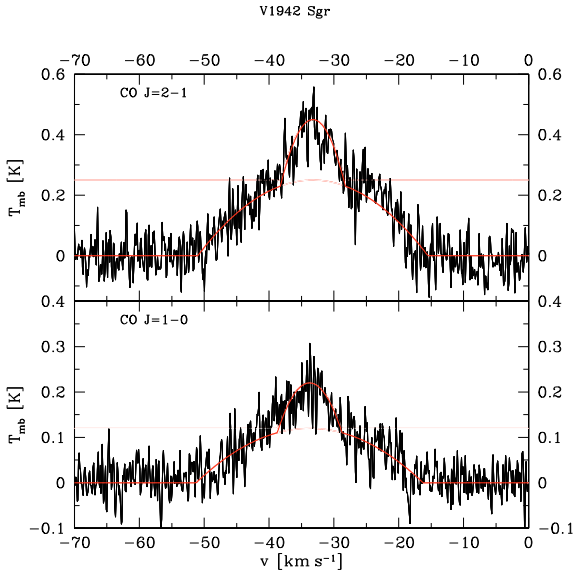

Fig. 4. CO (2–1, *upper panel*) and (1–0, *lower panel*) spectra of V1942 Sgr obtained with the IRAM-30 m telescope. The fits used to derive the wind parameters are also shown (see Table 1).

Each line profile was fitted with two parabolae to derive representative expansion velocities (Table 1). We estimate the mass-loss rates and photodissociation radii associated with each component using the same approach as in Winters et al. (2003). We adopt a CO/H mass ratio of 1 × 10^{-3}. The differences in the

Table 1. CO line parameters of V1942 Sgr.

	$V_{\rm lsr}$ km s^{-1}	$V_{\rm exp}$ km s^{-1}	$T_{\rm mb}$ K	$\dot{M}$ $M_\odot$ yr^{-1}	$R_{\rm CO}$ 10^{16} cm
CO (1–0)	–33.75 (0.25)	17.5 (0.5)	0.12 (0.01)	6.1 (0.3) 10^{-7}	6.9 (0.2)
	–33.75 (0.25)	5.0 (0.5)	0.10 (0.01)	1.0 (0.1) 10^{-7}	4.0 (0.2)
CO (2–1)	–33.25 (0.25)	17.75 (0.5)	0.25 (0.02)	4.3 (0.3) 10^{-7}	5.7 (0.2)
	–33.25 (0.25)	5.0 (0.5)	0.20 (0.02)	6.9 (0.5) 10^{-8}	3.2 (0.2)

Notes. Formal uncertainties are given in parentheses.

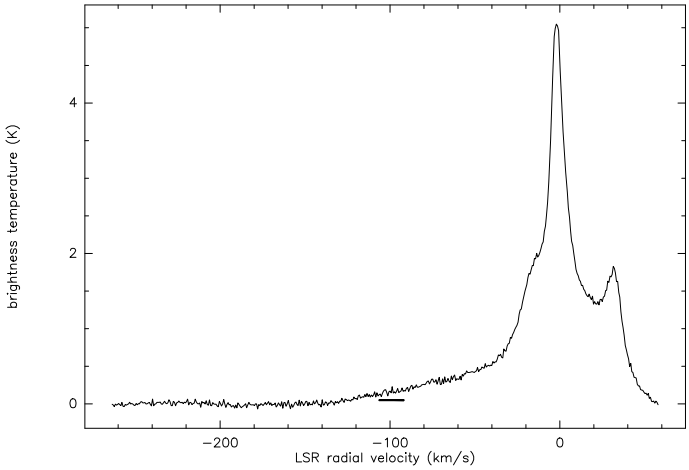

Fig. 5. Frequency-switch H I 21 cm spectrum obtained with the NRT on the position of V CrB. The bar indicates the velocity range of the CO emission.

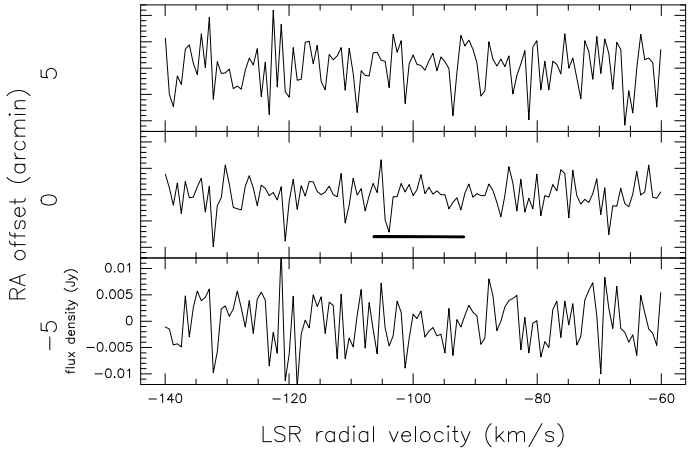

Fig. 6. H I spectra obtained for V CrB (*middle*), at +5′ east (*top*) and −5′ west (*bottom*) after correction for interstellar contamination (Sect. 3). The spectra have been smoothed to a resolution of 0.64 km s^{-1}. The bar indicates the velocity range of the CO emission.

mass-loss rates and photodissociation radii estimated from the two lines are comparable to the uncertainties in the fits.

3. V CrB

V CrB is a metal-poor ([M/H] = −1.35) carbon star on the TP-AGB with a C/O ratio around 1.10 (Abia et al. 2001). It is a Mira of period 358 days. Using the period-luminosity relation for carbon Miras of Whitelock et al. (2006), Guandalini (2009, in prep) determines a luminosity of 5600 $L_\odot$ and a distance of 547 pc. The temperature $T_{\rm eff}$ is estimated to be 2090 K (Bergeat et al. 2001). At such a low temperature (i.e., less than 2500 K), molecular hydrogen is expected to be the dominant species in the atmosphere and in the inner envelope of V CrB (Glassgold & Huggins 1983). Indeed, photospheric H_2 has been detected in the near-infrared (2.122 μm) by Johnson et al. (1983). This Mira is presently undergoing mass loss, since, for instance, it exhibits clear SiC dust emission at 11.3 μm (Goebel et al. 1981). The source has also been detected in the CO(1–0) and CO(2–1) rotational lines by Olofsson et al. (1993a), and more recently in CO(3–2) by Knapp et al. (1998). In contrast to V1942 Sgr, only one velocity component is visible. The central velocity is at $V_{\rm lsr}$ = −99.0 km s^{-1}, the expansion velocity, $V_{\rm exp}$ = 6.5 km s^{-1}, and the mass-loss rate, $\dot{M} \sim 2.1 \times 10^{-7}\ M_\odot$ yr^{-1} (at 547 pc). With the Plateau-de-Bure IRAM interferometer, Neri et al. (1998) measured a source size of 7″ in CO (1–0). On the other hand, IRAS has not detected extended far-infrared emission associated with V CrB (Young et al. 1993a, their Table 1).

V CrB was also observed for a total of 44 h in H I with the NRT. The frequency-switched spectrum shows no feature around the expected velocity of −99.0 km s^{-1} (Fig. 5), and only weak interstellar emission of at most 0.2 K around −99 km s^{-1}.

We obtained H I data in the position-switch mode of observation with off-positions at ±4′, ±6′, ±8′, ±10′, ±12′, ±16′, ±24′, and ±32′. As for V1942 Sgr we find that the interstellar emission varies linearly with offset, in the velocity range from −120 to −80 km s^{-1}. We are thus confident that the interstellar contamination can be corrected for accurately. The source is not detected at the star's position and at ±5′ in RA (Fig. 6, in which we have averaged the spectra obtained at +4′ and +6′, and at −4′ and −6′, to improve the sensitivity). By integrating over the velocity range defined by the CO emission (i.e., −106 to −92 km s^{-1}), an upper limit of 4 mJy × km s^{-1} can be set on the intensity of the H I emission at the V CrB's position in the area defined by the 4′ × 22′ NRT beam. This translates to an upper limit of $3 \times 10^{-4}\ M_\odot$ in atomic hydrogen at 547 pc. Since the source was not found to be extended by IRAS, we do not expect to find much material outside the NRT beam.

4. Interpretation

4.1. V1942 Sgr

The CO line profiles observed in V1942 Sgr have a characteristic composite profile. This kind of profile has been interpreted as evidence of a succession of mass-loss events with different outflow velocities by Knapp et al. (1998) and Winters et al. (2003). However, the interferometric data obtained for EP Aqr, a source with such profiles, are difficult to explain with this scenario (Winters et al. 2007). Furthermore, in other cases, X Her (Kahane & Jura 1996) and RS Cnc (Libert et al. 2009), there is evidence that the broad components originate in a bipolar flow. Bipolar flows are believed to develop at the end of the

AGB phase when the stars are about to begin their evolution towards the planetary nebula phase (e.g., Sahai et al. 2007).

The H I spectrum obtained at the star's position shows a pedestal of width 10 km s^{-1} that could be a counterpart to the narrow CO (1–0 and 2–1) components that have about the same width. The mass in hydrogen corresponding to this pedestal is $\sim 4 \times 10^{-3}$ $M_\odot$. Assuming 90% in H and 10% in ^{4}He, in number (i.e. a mean molecular weight, μ, of 1.3), and adopting a mass-loss rate of 1×10^{-7} $M_\odot$ yr^{-1} on the basis of the narrow CO components (see Table 1), the timescale would be 6×10^4 years, and the radius 0.31 pc ($\equiv 2'$). The stellar effective temperature (2960 K) is high enough for us to expect that most of the hydrogen is in atomic form.

On the other hand, there is no H I counterpart to the broad CO components at a level of 2 mJy. This seems to indicate that the broad components correspond to a quite recent phenomenon. Adopting an upper limit of 2 mJy, the flux is <0.07 Jy × km s^{-1}, and the mass in atomic hydrogen is at most 5×10^{-3} $M_\odot$. The timescale is then $\lesssim 10^4$ years.

The H I spectra obtained on V1942 Sgr are very similar to those obtained by Le Bertre & Gérard (2004) and Libert et al. (2007) on Y CVn, a well-documented carbon star with a detached shell discovered by IRAS (Young et al. 1993a) and imaged by ISO (Izumiura et al. 1996). At the central position, we detect a pedestal of width 10 km s^{-1}, twice the expansion velocity measured for the narrow CO components. At all positions, we detect a narrow line of width, $FWHM \sim 3$ km s^{-1}. This narrow profile proves that the stellar wind from V1942 Sgr is decelerated at some distance from the central star. Young et al. (1993b) interpreted the detached shells detected by IRAS at 60 μm as the effects of a slowing-down of stellar outflows by the surrounding interstellar matter. Elaborating on this hypothesis and using the formalism of Lamers & Cassinelli (1999), Libert et al. (2007) developed a model in which the inner radius of a detached shell corresponds to the location where the stellar wind is abruptly slowed down from $V_{\rm exp}$ to $\sim V_{\rm exp}/4$. The outer radius corresponds to the location where external matter is compressed by the expanding shell (bow shock). They applied this model to Y CVn and obtained excellent fits to the H I line profiles observed at different pointings, on and around the star's position.

We use the same model for V1942 Sgr. For the freely expanding wind ($r < r_1$), we adopt a velocity of 5.0 km s^{-1}, i.e., half the width of the pedestal, which also corresponds to the narrow CO components. The broad CO components have no obvious counterpart in H I. They probably trace a short-lived structure restricted to the central part of the circumstellar shell that has no effect on the large scales probed at 21 cm. The mass-loss rate, $\dot{M} = 1.0 \times 10^{-7}$ $M_\odot$ yr^{-1}, is adopted from the CO line fitting (Table 1). The central velocity is taken to be −32.9 km s^{-1}.

We obtain a good fit to the different H I line profiles (Figs. 2 and 7) with the parameters given in Table 2. The external radius, $r_2 \sim 3'$, that we have adopted is compatible with that derived by Young et al. (1993a) from IRAS data at 60 μm, $r_{\rm ext} \sim 3.2'$, but not the internal radius ($r_1 = 2'$ versus $r_{\rm int} \sim 0.2'$). In our model, r_1 is constrained by the parameters obtained from the low velocity CO components and by the intensity of the H I pedestal. We assume that the inner shell is too small compared to the IRAS beam at 60 μm ($FWHM \sim 2'$) to have been reliably constrained.

Table 2. Model parameters (d = 535 pc).

$\dot{M}$ (in hydrogen)	0.69×10^{-7} $M_\odot$ yr^{-1}
μ	1.3
t_1	61×10^3 years
$t_{\rm DS}$	5.4×10^5 years
r_1	0.31 pc (2.0′)
$r_{\rm f}$	0.41 pc (2.64′)
r_2	0.47 pc (3.0′)
$T_0(\equiv T_1^-)$, T_1^+	20 K, 746 K
$T_{\rm f}$ (=T_2)	81 K
$v_0(\equiv v_1^-)$, v_1^+	5.0 km s^{-1}, 1.27 km s^{-1}
$v_{\rm f}$	0.066 km s^{-1}
v_2	0.52 km s^{-1}
n_1^-, n_1^+	0.45 H cm^{-3}, 1.8 H cm^{-3}
$n_{\rm f}^-$, $n_{\rm f}^+$	21.0 H cm^{-3}, 2.15 H cm^{-3}
n_2	1.66 H cm^{-3}
$M_{r<r_1}$ (in hydrogen)	4.2×10^{-3} $M_\odot$
$M_{\rm DT,CS}$ (in hydrogen)	3.7×10^{-2} $M_\odot$
$M_{\rm DT,EX}$ (in hydrogen)	6.3×10^{-3} $M_\odot$

Notes. The notations are as in Libert et al. (2007). In particular, $t_{\rm DS}$ is the formation time of the detached shell, $M_{\rm DT,CS}$ is the mass of the circumstellar component of the detached shell, and $M_{\rm DT,EX}$ is the external mass accreted in the detached shell.

4.2. V CrB

V CrB was not detected in H I. Since there is no significant Galactic confusion, we are quite confident in our upper limit of 3×10^{-4} $M_\odot$ in atomic hydrogen. For a source losing atomic hydrogen with a mass-loss rate of 2.1×10^{-7} $M_\odot$ yr^{-1}, this would correspond to a timescale of 2000 years ($\mu = 1.3$). However, the stellar effective temperature is so low (2090 K) that hydrogen should be in molecular form in the atmosphere and outwards (Glassgold & Huggins 1983), until it is photodissociated by the interstellar radiation field. To estimate the distance, $R_{\rm ph}$, at which this happens, we follow the approach of Morris & Jura (1983). Assuming a mean intensity for the ultraviolet radiation between 912 and 1100 Å of 1.9×10^6 photons cm^{-2} s^{-1} sr^{-1}, and that 0.11 of all absorptions lead to a dissociation, we infer that $R_{\rm ph} \sim 410\,\dot{M}^{1/2}$, where $R_{\rm ph}$ is in pc and $\dot{M}$ in $M_\odot$ yr^{-1}. For a mass-loss rate of 2.1×10^{-7} $M_\odot$ yr^{-1}, we obtain $R_{\rm ph} = 0.2$ pc ($\equiv 1.2'$), which corresponds to a dynamical time of $\approx 3 \times 10^4$ years ($V_{\rm exp} = 6.5$ km s^{-1}).

Therefore, the non-detection of V CrB in H I implies that it has not been undergoing mass loss at the present rate for more than 3.2×10^4 years. Furthermore, when comparing with V1942 Sgr, which is at the same distance, we can state that V CrB has not experienced the same phase of mass loss during the past 5×10^5 years, because if it had it would have been easily detected in a way similar to V1942 Sgr.

This reasoning assumes that molecular hydrogen is not self-protected within small-scale structures that might develop in the stellar outflow. However, the non-detection by IRAS of an extended emission around V CrB (Young et al. 1993a) is consistent with our conclusion that mass loss started only recently.

4.3. Discussion

The V1942 Sgr proper motion measured by Hipparcos is 10.98 mas yr^{-1} in RA and −5.10 mas yr^{-1} in Dec. When corrected for solar motion towards apex and for a distance of 535 pc, it translates to 6.45 mas in RA and −2.28 mas in Dec. This implies a motion in the plane of the sky at a velocity of 17 km s^{-1}, at a position angle, PA = 110°. Accounting for the radial velocity, $V_{\rm lsr} = -33$ km s^{-1}, we obtain a 3D space velocity of 37 km s^{-1}. The offset with respect to the central star that we find in the H I map might therefore be an effect of the motion of V1942 Sgr

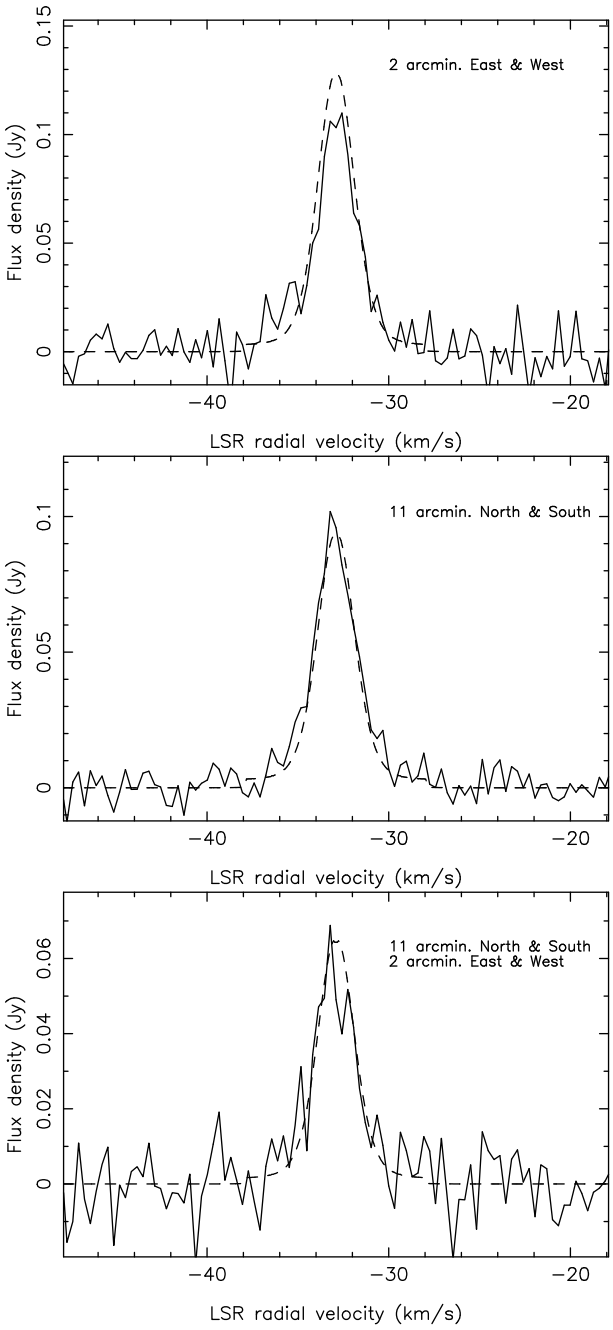

Fig. 7. Comparison between the H I line profiles obtained on V1942 Sgr and the detached-shell model discussed in Sect. 4.1. *Top*: average of the two spectra at +2′ (east) and −2′ (west). *Middle*: average of the two spectra at +11′ (north) and −11′ (south). *Bottom*: average of the four spectra at (+2′, +11′), (–2′, +11′), (+2′, –11′), and (–2′, –11′).

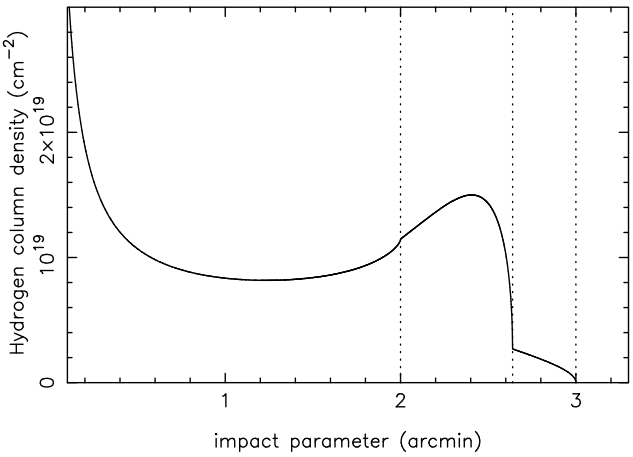

Fig. 8. Atomic hydrogen column density profile for the V1942 Sgr model. The vertical lines mark the radii r_1 (0.31 pc), r_f (0.41 pc), and r_2 (0.47 pc), which define the detached shell.

relative to the surrounding ISM. Such a deformation in H I has already been noted in several cases: Mira (Matthews et al. 2008), RX Lep (Libert et al. 2008), and RS Cnc (MR2007 and Libert et al. 2009). GL2006 noted also that many H I sources are offset with respect to the central stars. A visual inspection of the IRAS map at 60 μm of V1942 Sgr (after the Improved Reprocessing of the IRAS Survey: Miville-Deschênes & Lagache 2005) indicates that the image is slightly elongated in RA and shifted west by ∼1/2 pixel (≡0.75′), in agreement with our H I map. Finally, we note that the central velocity in H I is −32.9 ± 0.3 km s^{-1}, whereas in CO it is −33.5 ± 0.25 km s^{-1}. This effect is small but consistent with an interaction between the external shell of V1942 Sgr and its local ISM. Shifts in velocity of the H I emission towards the LSR have already been reported in several red giants (GL2006, Matthews et al. 2008).

From their study of circumstellar shells resolved by IRAS, Young et al. (1993b) find that, among nearby AGB stars detected in CO, Miras, in contrast to semi-regulars, are in general unresolved. They suggest that the latter have been losing matter for a longer time than the former. In their H I survey of evolved stars, GL2006 obtained results that agree with this suggestion. Although their sample is small, several Miras with high mass-loss rates could not be detected in H I, whereas SRs were often easily detected. The high quality data that we have obtained for V1942 Sgr and V CrB strengthen the case of SRs undergoing mass loss for a longer time than Miras. One normally assumes that SRs evolve into Miras, and it is puzzling to find no relics of this SR phase around several Miras. SRs might evolve directly in the post-AGB phase, as suggested also by the presence of bipolar outflows that has been reported in several cases (Kahane & Jura 1996; Libert et al. 2009).

Young et al. (1993b) also find that extended sources are observed preferentially around carbon stars and GL2006 obtained a higher rate of detection of carbon stars in H I. However, the case of V CrB seems to suggest that some stars could reach the carbon-rich stage without undergoing substantial mass loss previously. In a systematic investigation of the relations between mass loss and red giant characterstics, Winters et al. (2000) find that the mass-loss rate depends critically on stellar parameters such as the effective temperature, which controls the dust formation, and the luminosity, which controls the radiation pressure. V CrB may have switched only recently from the B-regime (with a low and, presently, undetected wind) to the A-regime with a wind at a few 10^{-7} $M_\odot$ yr^{-1}.

Although both V1942 Sgr and V CrB are carbon stars on the TP-AGB phase, their history of mass loss during the past 5×10^5 years seem to differ dramatically. If it is correct that the bipolar shaping is a signpost of the end of the AGB, V1942 Sgr (and also sources with composite CO line profiles) might be on the verge of leaving this phase. Both sources have similar C/O abundance ratios, 1.12 for V1942 Sgr (Olofsson et al. 1993b) and 1.10 for V CrB (Abia et al. 2001), and similar luminosities, 5200 and 5600 $L_\odot$, respectively. Both sources also have a low ^{12}C/^{13}C abundance ratio, 30 for V1942 Sgr (Abia & Isern 1997) and 10 for V CrB (Abia et al. 2001), compared to ∼40 for

the majority of carbon stars in the AGB phase. The explanation of these low abundance ratios is not known, but could be due to a non-standard mixing process occurring in low-mass stars at the base of the convective stellar envelope ("cool bottom processing", Nollett et al. 2003).

5. Conclusions

The combination of high velocity resolution CO and H I data provides a promising tool to investigate the history of mass loss by evolved stars. The low level of Galactic H I emission and the absence of small-scale structure in this emission have allowed us to obtain H I data of high quality for V1942 Sgr and V CrB with the NRT. We have also obtained high quality CO (1–0) and (2–1) spectra of V1942 Sgr with the IRAM 30-m telescope.

For V1942 Sgr, the CO spectra exhibit composite profiles revealing a low velocity wind of $\sim 10^{-7}\ M_\odot\ \mathrm{yr}^{-1}$ and a high velocity wind, possibly bipolar, of $\sim 5 \times 10^{-7}\ M_\odot\ \mathrm{yr}^{-1}$. A comparison with the H I spectrum shows that this high velocity wind is recent with an age of at most 10^4 years. On the other hand, the low velocity wind appears to have filled a cavity of ~0.2 pc in radius and created the detached shell, which was discovered by IRAS, over a period of 5×10^5 years. Follow-up observations with the VLA and ALMA would help us to refine this scenario, or possibly develop a new scheme. The narrowness of the H I line profile in V1942 Sgr provides new evidence that AGB stellar winds are slowed down by their surrounding medium, as surmised by Young et al. (1993b).

For V CrB, the CO spectra that have been published reveal an outflow with expansion velocity, 6.5 km s^{-1}, and mass-loss rate, $2.1 \times 10^{-7}\ M_\odot\ \mathrm{yr}^{-1}$. The non-detection in H I of V CrB places an upper limit of 3.2×10^4 years on the age of this outflow. In the case of a star with low effective temperature, molecular hydrogen data are obviously needed to constrain the history of mass loss more accurately.

Acknowledgements. The Nançay Radio Observatory is the Unité scientifique de Nançay of the Observatoire de Paris, associated as Unité de Service et de Recherche (USR) No. B704 to the French Centre National de la Recherche Scientifique (CNRS). The Nançay Observatory also gratefully acknowledges the financial support of the Conseil Régional de la Région Centre in France. We thank the IRAM Director, P. Cox, for allowing the CO observations of V1942 Sgr to be made on Director's time (D01-09). IRAM is supported by INSU/CNRS (France), MPG (Germany), and IGN (Spain). We are grateful to C. Abia, M. Busso, R. Guandalini, and A. Jorissen for enlightening discussions, and to the referee for careful comments that helped us to improve the manuscript. This research has made use of the SIMBAD and VizieR databases, operated at CDS, Strasbourg, France and of the NASA's Astrophysics Data System.

References

Abia, C., & Isern, J. 1997, MNRAS, 289, L11
Abia, C., Busso, M., Gallino, R., et al. 2001, ApJ, 559, 1117
Bergeat, J., Knapik, A., & Rutily, B. 2001, A&A, 369, 178
Gérard, E., & Le Bertre, T. 2006, AJ, 132, 2566 (GL2006)
Glassgold, A. E., & Huggins, P. J. 1983, MNRAS, 203, 517
Goebel, J. H., Bregman, J. D., Witteborn, F. C., Taylor, B. J., & Willner, S. P. 1981, ApJ, 246, 455
Izumiura, H., Hashimoto, O., Kawara, K., Yamamura, I., & Waters, L. B. F. M. 1996, A&A, 315, L221
Johnson, H. R., Goebel, J. H., Goorvitch, D., & Ridgway, S. T. 1983, ApJ, 270, L63
Kahane, C., & Jura, M. 1996, A&A, 310, 952
Knapp, G. R., Young, K., Lee, E., & Jorissen, A. 1998, ApJS, 117, 209
Lamers, J. G. L. M., & Cassinelli, J. P. 1999, Introduction to Stellar Winds (Cambridge University Press)
Le Bertre, T., & Gérard, E. 2004, A&A, 419, 549
Lebzelter, T., & Obbrugger, M. 2009, Astron. Nachr., 330, 390
Libert, Y., Gérard, E., & Le Bertre, T. 2007, MNRAS, 380, 1161
Libert, Y., Le Bertre, T., Gérard, E., & Winters, J. M. 2008, A&A, 491, 789
Libert, Y., Winters, J. M., Le Bertre, T., Gérard, E., & Matthews, L. D. 2009, A&A, submitted
Matthews, L. D., & Reid, M. J., 2007, AJ, 133, 2291 (MR2007)
Matthews, L. D., Libert, Y., Gérard, E., Le Bertre, T., & Reid, M. J. 2008, ApJ, 684, 603
Miville-Deschênes, M.-A., & Lagache, G. 2005, ApJS, 157, 302
Morris, M., & Jura, M. 1983, ApJ, 264, 546
Neri, R., Kahane, C., Lucas, R., Bujarrabal, V., & Loup, C. 1998, A&AS, 130, 1
Nollett, K. M., Busso, M., & Wasserburg, G. J. 2003, ApJ, 582, 1036
Olofsson, H. 1999, IAU Symp., 191, 3
Olofsson, H., Eriksson, K., Gustafsson, B., & Carlström, U. 1993a, ApJS, 87, 267
Olofsson, H., Eriksson, K., Gustafsson, B., & Carlström, U. 1993b, ApJS, 87, 305
Reich, P., & Reich, W. 1986, A&AS, 63, 205
Sahai, R., Morris, M., Sánchez Contreras, C., & Claussen, M. 2007, AJ, 134, 2200
Schöier, F. L., & Olofsson, H. 2001, A&A, 368, 969
van Leeuwen, F. 2007, Hipparcos, the New Reduction of the Raw Data (Springer), Astrophysics and Space Science Library, 350
Whitelock, P. A., Feast, M. W., Marang, F., & Groenewegen, M. A. T. 2006, MNRAS, 369, 751
Winters, J. M., Le Bertre, T., Jeong, K. S., Helling, C., & Sedlmayr, E. 2000, A&A, 361, 641
Winters, J. M., Le Bertre, T., Jeong, K. S., Nyman, L.-Å., & Epchtein, N. 2003, A&A, 409, 715
Winters, J. M., Le Bertre, T., Pety, J., & Neri, R. 2007, A&A, 475, 559
Young, K., Phillips, T. G., & Knapp, G. R. 1993a, ApJS, 86, 517
Young, K., Phillips, T. G., & Knapp, G. R. 1993b, ApJ, 409, 725